Surface integrity in micro-grinding of Ti6Al4V considering the specific micro-grinding energy

Available online at www.sciencedirect.com

ScienceDirect

Procedia CIRP 87 (2020) 181–185

www.elsevier.com/locate/procedia

5th CIRP CSI 2020

Surface integrity in micro-grinding of Ti6Al4V considering the specific micro-grinding energy

Mohammadali Kadivar [a,b*], Bahman Azarhoushang[a], Amir Daneshi[a], Peter Krajnik[b]

[a]*Institute for Precision Machining (KSF), Furtwangen University of Applied Sciences, Jakob-Kienzle-Str 17, 78056 Villingen-Schwenningen, Germany*

[b]*Department of Industrial and Materials Science, Chalmers University of Technology, Hörsalsvägen 7B, SE-412 96 Gothenburg, Sweden*

* Corresponding author. Tel.: +49 746115026723; fax: +49 7720 955779. *E-mail address:* Kamo@hs-furtwangen.de

Abstract

Surface integrity is one of the most significant quality aspects of micro-grinding of difficult-to-cut materials. On the other hand, specific grinding energy is a fundamental parameter for describing the micro-grinding process. This paper addresses the surface integrity of the micro-ground surface of a titanium alloy under different cutting speeds and feed-rate-to-depth-of-cut (v_w/a_e) ratios at the same chip thickness. Three different cutting speeds and v_w/a_e ratios have been chosen and the residual stress of the workpiece, as well as the specific micro-grinding energy, have been investigated. The results showed that almost the same minimum specific grinding energy was obtained at tested cutting speed and v_w/a_e ratio. The results of the XRD analysis showed that contrary to the specific micro-grinding energy, the residual stresses of the ground surface changed by varying the cutting speed and v_w/a_e ratio. Higher cutting speeds resulted in lower compressive residual stress, and higher v_w/a_e ratios resulted in higher compressive stresses. This can be attributed to higher temperatures in the chip-formation process compared to the plastic deformation in micro-grinding at higher cutting speeds and lower v_w/a_e ratios which was proved via SEM micrographs.

Keywords: Surface integrity; micro-grinding; titanium

1. Introduction

In comparison to other bio-materials, like ceramics and germanium, Ti6Al4V (titanium grade 5) is a promising material for biomedical and aerospace industries which require extraordinary properties [1]. Due to the hard nature of titanium, fabrication of damage-free surfaces is challenging, and its machining is always accompanied by high plastic deformation due to high cutting forces and rapid tool wear. The micro-grinding process is a promising material removal method when high form and dimensional accuracies and fine finished surfaces with no or minimal damages are. During the micro-grinding process, the elastic and plastic deformations, chip formation and friction between the grains and the workpiece material result in relatively high specific energy which is required to remove the material. The generated specific energy of micro-grinding can be described as a closely correlated parameter to the ground surface integrity. It is hence a fundamental parameter/indicator to assess the grindability of the material. The mechanical work during the material removal process results in compressive residual stresses, while the cutting temperature over the surface of the material results in tensile residual stresses, which may cause surface and sub-surface damages. These damages negatively affect the performance of the parts. Therefore, connecting the specific grinding energy to the integrity of the finished surface is essential.

Gong et al. [2] and Zhou et al. [3] analyzed the removal mechanism of nickel-based single crystal superalloy and developed a prediction model for the micro-grinding forces. They also studied the effect of grinding parameters on grinding forces and microstructure of ground surface and sub-surface.

10.1016/j.procir.2020.02.069

They showed that the most shear slipping planes of nickel-based single crystal superalloy are {111} planes. The thickness of subsurface plastic deformation and the surface roughness increased with increasing the feed rate and grinding depth and decreased with increasing the cutting speed. Kadivar et al. [4] showed that the surface roughness of the ground surface in micro-grinding of Ti-6Al-4V is highly connected to the dressing and grinding parameters.

Based on the experimental work of Fook et al. [5], low peripheral speed and low depth of cut are the main parameters to achieve optimum surface integrity while micro-grinding of bioceramics. Zhang et al. [6,7] studied the surface integrity of amorphized Si during micro-grinding of RB-SiC/Si composites. They showed that the recrystallization developed at higher feed rates. At lower feed rates, the surface generation mechanism changed from micro-breaking to smoother surface. Morgan et al. [8] studied the specific energy of micro-grinding while grinding tungsten carbide. They showed that the grinding specific energy dropped suddenly and then remained constant after the tool engagement.

The number of publications with a focus on the specific energy of micro-grinding and its connection to the surface integrity is limited. There are very few studies with the focus on the micro-grinding of titanium alloys. To fulfill this research gap, Ti6Al4V titanium was ground at the same chip thicknesses with different cutting speeds and feed rate-to-depth of cut ratios, and the surface integrity was analyzed by XRD and SEM techniques.

2. Methodology

The micro-grinding of Ti6Al4V titanium alloy was carried out on a high-precision micro-grinding machine (Kern Pyrimad Nano) with grinding oil as the lubricant. A vitrified diamond micro-tool with a diameter of 2 mm, a diamond grain size of 46, and a concentration of 150 was used for the experiments. The grinding tool was dressed prior to each test using a diamond rotary dresser with dressing overlap ratio, U_d, of 2, dressing speed ratio, q_d, of +0.8, and a constant dressing depth of cut, a_{ed}, 2 µm. The micro-grinding tests were conducted at three different cutting speeds (v_c) and feed-rate-to-depth-of-cut ratios (v_w/a_e) while keeping the equivalent chip thickness at a constant level. For the sake of repeatability, each test was repeated two times. Table 1 lists the used grinding parameters. The normal and tangential grinding forces were measured using a type 9256C2 Kistler dynamometer. The experimental setup is shown in Fig. 1. The surface integrity of the parts was analyzed using SEM with the penetration depth of the radiation of 5 µm and XRD techniques. Prior to each trial, each workpiece was 50 µm ground with conservative grinding parameters (a_e = 1µm, v_w = 50 mm/min and v_c = 6 m/s), inducing low grinding forces and temperature.

Table 1. Experimental parameters

Cutting speed (v_c)	6, 10, and 14 m/s
Maximum chip thickness (h_{cu})	0.5, 1.3, 2.3 and 2.9 µm
Feed rate to depth of cut ratio (v_w/a_e)	5, 8, and 11 x10^4
Axial depth of cut (a_p)	3.5 mm

The maximum chip thickness, h_{cu}, has been used in this study to compare the results. The maximum chip thickness, in practice, depends on the cutting-edge density and grit shape factor. To calculate the h_{cu}, probabilistic modeling was used [9]. All the number of abrasive grains over the whole surface of the grinding tool was counted in different heights using a confocal microscope. The density of dynamic cutting edges, the real tool-workpiece contact length and maximum chip thickness were calculated based on this probabilistic analysis method. The calculation method can be found in [9].

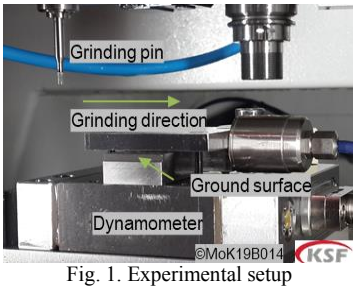

Fig. 1. Experimental setup

The specific grinding energy, e_c, indicates the process efficiency and depends on the grinding parameters such as grinding power and material removal rate and is given by [10]:

$$e_c = \frac{F_t\, v_c}{a_p\, a_e\, v_w} = \frac{F_t\, v_c}{Q_w} \qquad (2)$$

where a_p is the axial depth of cut, F_t is the tangential grinding force, and Q_w represents the material removal rate.

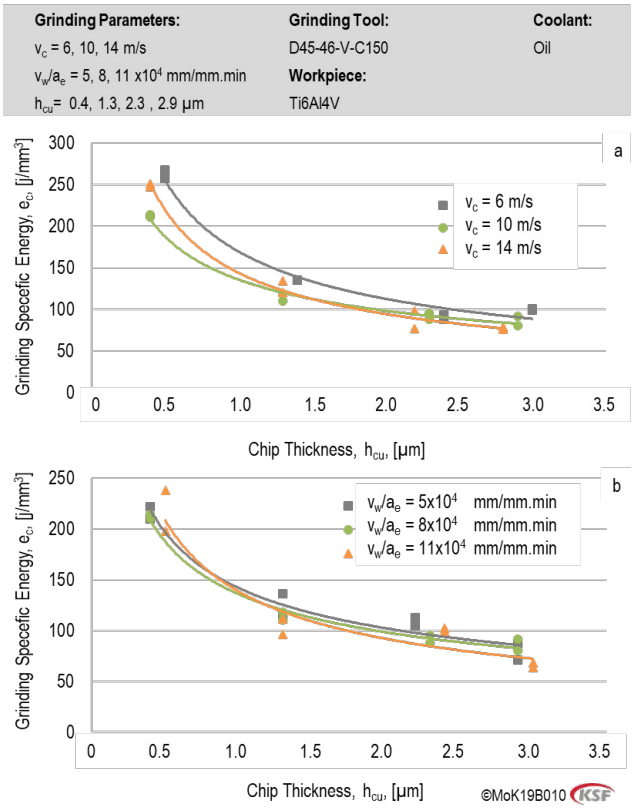

Fig. 2. The grinding specific energy versus maximum undeformed chip thickness. (a) the effect of cutting speed (v_w/a_e = 8x10^4 mm/mm.min); (b) the effect of feed-rate-to-depth-of-cut ratio (v_c = 10 m/s)

3. Results and discussion

Fig. 2 illustrates the effect of different cutting speeds and feed-rate-to-depth-of-cut ratios on specific energy. With increasing chip thickness, the shares of friction and plastic deformation in chip formation decrease and consequently the grinding process becomes more efficient. With this, the specific grinding energy approaches its minimum value (between 12-15 J/mm^3 [11,12]). Reaching the minimum specific grinding energy (e.g. values common/associated with conventional/macro grinding of same materials) via micro-grinding process is not probable since this minimum value can only be achieved by high values of the chip thickness in the grinding process (utilizing high depth of cuts and feed rates). Duo to the nature of the micro-grinding process, i.e. small tool diameter and high tool deflection, achieving high values of the chip thickness is practically impossible. Using lower cutting speeds led to higher specific grinding energy. Interestingly changing the cutting speed from 10 to 14 m/s did not change the value of the specific grinding energy considerably. The reason may because of the process temperature and also chip formation mechanisms at different cutting speeds which need to be investigated fundamentally.

Changing the cutting speed may vary shares of the friction and plastic deformation in the chip formation process due to inertia effects and/or influence of the chip thickness. This can be perceived via the obtained specific energy values. A lower share of plowing and friction promotes a more efficient grinding process and a higher share of the cutting action. According to Fig. 2a, the highest values of the specific energy occurred at a cutting speed of 6 m/s. The specific grinding energies are in the same order for the cutting speeds of 10 and 14 m/s. For a better understanding, an SEM investigation is required to study the effect of the cutting speed on the surface quality and process efficiency.

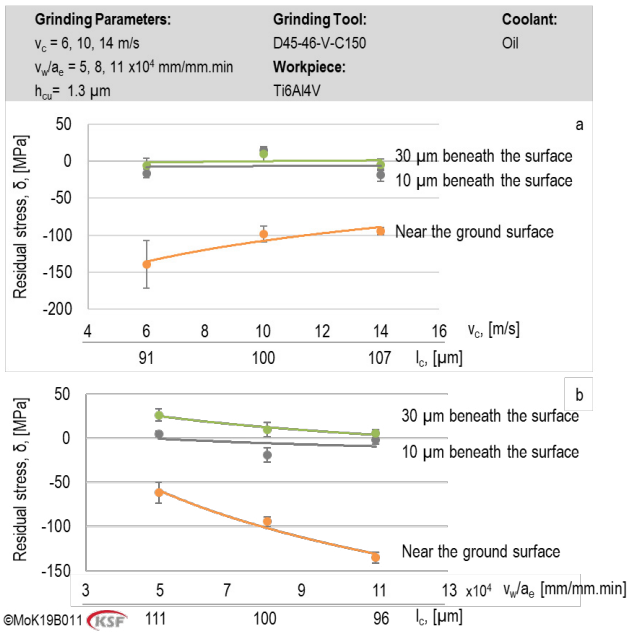

Fig. 3. The residual stress at constant chip thickness versus (a) the cutting speed (v_w/a_e = 8x10^4); (b) the feed rate to depth of cut ratio (v_c = 10 m/s)

Fig. 2b shows the effect of the feed-rate-to-depth-of-cut ratio on the specific grinding energy. Increasing this ratio did not result in variation of the specific grinding energy – meaning the independency of the process efficiency to the v_w/a_e ratio.

In the grinding process, the induced residual stress arises as a result of the thermo-mechanical effects during the material removal process. They can be related either to thermal or mechanical loads. Thermal loads, such as the thermo-plastic deformation at elevated temperatures, lead to tensile residual stresses – in this case, due to limited material expansion as a result of high temperature occurring in a very short time period and the rapid cooling in the contact zone. Mechanical loads, like the mechanical and plastic deformation loads on the ground surface, cause compressive residual stresses [13–16].

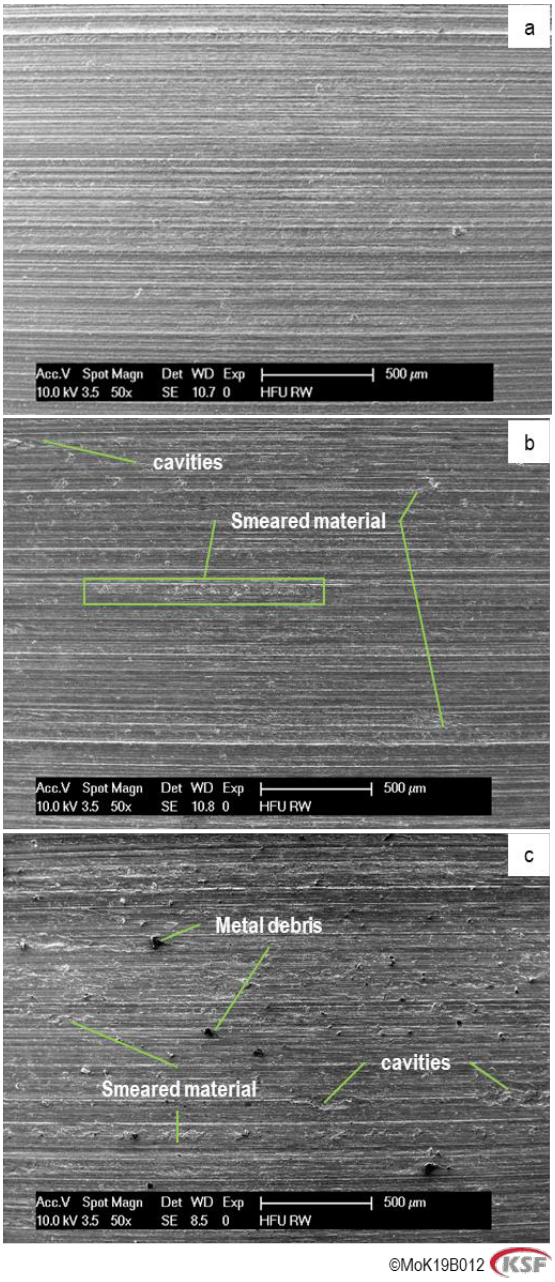

Fig. 4. SEM pictures of the ground surface at different cutting speeds but constant chip thickness (a) v_c = 6 m/s; (b) v_c = 10 m/s; (c) v_c = 14 m/s (v_w/a_e = 8x10^4 mm/mm.min and h_{cu}= 1.3 µm)

Fig. 3 shows the results of residual stress measurement using the XRD technique. Compressive residual stresses were observed in all test specimens. In the micro-grinding process, the grinding temperature is low compared to the conventional/macro grinding process. Therefore, residual stresses are likely induced by mechanical loads which are the result of the mechanical load during the grinding process. Increasing the cutting speed from 6 m/s to 10 m/s resulted in lower compressive residual stresses. And increasing the cutting speed from 10 m/s to 14 m/s did not change the residual stresses significantly. The error bars show the repeatability of the test as it was mentioned each test was 2 times performed and the error bars show the domain of the result. Using a higher feed rate and lower depth of cut (higher v_w/a_e ratio) resulted in more compressive residual stress.

Fig. 4 illustrates the effect of cutting speed on the surface quality of the ground surface at a similar chip thickness (1.3 µm) and the feed-rate-to-depth-of-cut ratio of $8x10^4$ mm/mm.min. The results show that increasing the cutting speed deteriorated the surface quality of the workpiece. At a cutting speed of 6 m/s only the feed marks and grinding paths can be observed, and the surface is free of defects. Increasing the cutting speed to 10 m/s caused some amount of smeared material over the ground surface as well as some cavities – meaning more plastic deformation and possibly higher process temperature during the grinding process. Increasing the cutting speed to 14 m/s amplified surface errors as a result of high plastic deformation and higher temperatures compared to the cutting speed of 6 m/s. More cavities and large amounts of smeared material could be observed over the ground surface. Moreover, some material debris were found on the ground surfaces at higher cutting speeds. The results indicate that although the v_w/a_e ratio does not have a noticeable influence on the specific grinding energy, it can largely affect the residual stresses of the finished part, which is a novel finding.

The integrity of the ground surface is influenced by micro-grinding parameters i.e. cutting speed and v_w/a_e ratio. The residual stress can be generated due to thermal and/or mechanical stresses [17]. The thermal stress is responsible for tensile residual stress and the mechanical stress for compressive one. The measured residual stresses in Fig.3 indicate that they were generated only near the ground surface and beneath the surface the effects of neither thermal nor mechanical stresses were seen. In addition, no tensile residual stresses were generated on the ground surface, but compressive stresses up to around 150 MPa were measured. This confirms that the effect of mechanical loads on the surface is dominant and the heat generation in micro-grinding (in contrast to macro-grinding) is not so high that any tensile residual stress can be generated.

Figs. 2-4 suggest that the grinding specific energy can be connected to the surface integrity. Comparing Figs. 2a and 3b shows that where the specific micro-grinding energy is higher (v_c = 6 m/s) more compressive residual stress was induced. This is due to the higher mechanical loads (grinding forces) on the surface at v_c = 6 m/s compared to the higher cutting speeds. The residual stress values shown in Fig. 3a corresponds to the chip thickness of about 1.3 µm in Fig.2a. In order to keep the chip thickness constant, depth of cut and feed rate varied at different cutting speeds, resulting in a change in the tool-workpiece contact length (l_c). Hence, according to Fig.3a, rising the cutting speed from 6 to 10 m/s leads to a 10% increase in the contact length (l_c). The specific energy and consequently mechanical load on the ground surface at v_c = 6 m/s (at h_{cu} = 1.3 µm) is about 15% higher than that at v_c = 10 m/s. On the other hand, this increased force is distributed on the 10% smaller contact zone, as a result of which about 35% more compressive residual stress on the ground surface was generated. The same effect, but with a slighter trend, can be seen in Figs. 2a and 3a by increasing the cutting speed from 10 to 14m/s (almost the same specific energy, 7% larger l_c).

At the higher cutting speed and at a constant chip thickness, the number of wheel rotation during the grinding path increases (cutting speed 14 m/s about 2 times higher than cutting speed 6 m/s). Despite, lower heat generation at higher cutting speeds (e.g. v_c = 6 m/s compared to 10 and 14 m/s), due to the higher rotation number, the surface temperature can elevate. As a result, the surface quality became worse with cutting speed (Fig.4; more debris and smeared material at higher cutting speeds). The elevated surface temperature with an increase in cutting speed can principally induce tensile residual stresses if its order is big enough. Recognizing the contribution of thermal and compressive stresses on the values measured in Fig.3a needs further fundamental investigation.

Comparing Figs. 2b and 3b shows that the specific grinding energy is in the same order by varying the v_w/a_e ratio (at each constant chip thickness); the residual stresses changed with changing the v_w/a_e ratio. The almost constant grinding specific energies at various cutting speeds and the v_w/a_e ratios (at constant chip thicknesses) express that the tangential grinding forces are in the same order. Increasing the v_w/a_e ratio leads to a lower contact time between the tool and the workpiece (either due to a smaller contact length (Fig.3b.) or due to higher feed speeds, leading to a smaller heat partition into the workpiece. Thus, higher compressive residual stress was induced in $v_w/a_e = 11x10^4$ compared with $8x10^4$ and $5x10^4$.

Measuring the process temperature may lead to a better understanding of the effects of the process parameters on the surface integrity and the specific grinding energy. This is beyond the scope of current work but is planned in the future.

Conclusions

The surface integrity of Ti6Al4V in micro-grinding process considering the specific energy was studied. The combined effect of both material removal and plastic deformation has been considered, and the effects of the cutting speed and feed-rate-to-depth-of-cut ratio was studied. The following conclusions were drawn:

- Feed-rate-to-depth-of-cut ratio did not significantly change the value of the specific energy of micro-grinding while keeping the maximum chip thickness constant.

However, using lower cutting speeds resulted in higher specific grinding energy.

- Micro-grinding experiments induced only compressive residual stresses –limited to the ground surface. Lower cutting speed and higher v_w/a_e ratio resulted in larger compressive residual stresses. The induced compressive residual stresses by varying the v_w/a_e ratio were mostly as a result of thermal loads. Changing the cutting speed generated both thermal and mechanical loads.
- The tool-workpiece contact length plays an important role in induced residual stresses. At the same specific energies, changing the contact length results in different residual stresses.
- Almost a damage-free surface was achieved employing the cutting speed of 6 m/s. High cutting speeds led to a huge amount of smeared material, cavities, and material debris.
- To achieve a finished surface with good surface integrity, in a constant material removal rate, the lower cutting speed and higher feed rate instead of a large depth of cut are suggested.

Acknowledgments

The authors would like to acknowledge the Meister Abrasives AG for providing the micro-grinding tool, Ph.D. student Mr. Felix Blendinger for his time and effort to help us in SEM picturing, and Stresstech GmbH for measuring the residual stress. The authors would also thank the CohMed (BMBF) for funding this project with the funding code of 03FH5I03IA.

References

[1] Kadivar M. Micro-grinding of titanium. Licentiate thesis, Chalmers University of Technology; 2018.
[2] Gong Y, Zhou Y, Wen X, Cheng J, Sun Y, Ma L. Experimental study on micro-grinding force and subsurface microstructure of nickel-based single crystal superalloy in micro grinding. J Mech Sci Technol; 2017.31(7):3397–410.
[3] Zhou Y, Gong Y, Cai M, Zhu Z, Gao Q, Wen X. Study on surface quality and subsurface recrystallization of nickel-based single-crystal superalloy in micro-grinding. Int J Adv Manuf Technol; 2017. 90(5-8):1749–68.
[4] Kadivar M, Azarhoushang B, Shamray S, Krajnik P. The effect of dressing parameters on micro-grinding of titanium alloy. Precision Engineering; 2018. 51:176–85.
[5] Fook P, Berger D, Riemer O, Karpuschewski B. Structuring of Bioceramics by Micro-Grinding for Dental Implant Applications. Micromachines (Basel); 2019. 10(5).
[6] Zhang Q, To S, Zhao Q, Guo B. Recrystallization of amorphized Si during micro-grinding of RB-SiC/Si composites. Materials Letters; 2016. 172:48–51.
[7] Zhang Q, To S, Zhao Q, Guo B. Amorphization and C segregation based surface generation of Reaction-Bonded SiC/Si composites under micro-grinding. International Journal of Machine Tools and Manufacture; 2015. 95:78–81.
[8] Morgan CJ, Vallance RR, Marsh ER. Specific grinding energy while microgrinding tungsten carbide with polycrystalline diamond micro tools. In: ICOMM-2007 2nd International Conference on Micro-Manufacturing; 2007. p. 180–187.
[9] Daneshi A. Micro chip formation mechanism in grinding of Nickel-base superalloy-Inconel 718. Albert-Ludwigs-Universität Freiburg; 2019.
[10] Malkin S, Guo C. Grinding technology: theory and application of machining with abrasives. Industrial Press Inc; 2008.
[11] Guo GQ, Liu ZQ, Zheng XH, Chen M. Investigation on Surface Grinding of Ti-6Al-4V Using Minimum Quantity Lubrication. Advanced material research. 2012. 500:308–13.
[12] Kacalak W, Lipiński D, Bałasz B, Rypina Ł, Tandecka K, Szafraniec F. Performance evaluation of the grinding wheel with aggregates of grains in grinding of Ti-6Al-4V titanium alloy. Int J Adv Manuf Technol; 2018. 94(1-4):301–14.
[13] Brinksmeier E, Brockhoff T. Randschicht-wärmebehandlung durch schleifen. HTM. Härterei-technische Mitteilungen; 1994. 49(5):327–30.
[14] Capello E, Semeraro Q. Process Parameters and Residual Stresses in Cylindrical Grinding. J. Manuf. Sci. Eng.; 2002. 124(3):615.
[15] Nachmani Z. Randzonenbeeinflussung beim Schnellhubschleifen. Apprimus-Verlag; 2008.
[16] Azarhoushang B, Kadivar M, Bösinger R, Shamray S, Zahedi A, Daneshi A. High-speed high-efficient grinding of CMCs with structured grinding wheels. Int J Adv Manuf Technol; 2019. 9(1):1.
[17] Hamdi H, Zahouani H, Bergheau J. Residual stresses computation in a grinding process. Journal of Materials Processing Technology; 2004. 147(3):277–85.